

The Influence of RF Sputtering Power on Optical and Structural Properties of AlN Films for High Power Electronic Applications

Mohammad Asef Hossaini^a, Siti Sarah Saniman^a, Syariffah Nurathirah Syed Yaacob^a, Muhammad Firdaus Omar^{a*} and Azzahfeerah Mahyuddin^b

^aDepartment of Physics, Faculty of Science, Universiti Teknologi Malaysia, 81310 Johor Bahru, Johor, Malaysia

^bDepartment of Quality Engineering Universiti Kuala Lumpur Malaysian Institute of Industrial Technology, Persiaaran Sinaran Ilmu Bandar Seri Alam 81750, Johor Malaysia

(Received: 2.5.2023 ; Accepted: 19.2.2024 ; Published: 8.3.2024)

Abstract. The structural and optical properties Aluminum Nitride (AlN) thin film deposited is mainly influence by many depositions condition ie. RF sputtering power. In this work, the AlN thin films were synthesized on a silicon wafer as a substrate at ambient temperature under different RF sputtering power (150W, 175W, 200W, 225W, and 250W) by RF magnetron sputtering method. The influence of different RF sputtering power on crystal orientation and optical properties such as energy band gap on AlN thin films were examined using XRD, UV Vis spectroscopy. The analysis of the deposited AlN films revealed that the crystal quality and the optical bandgap of the AlN thin films increased as the RF sputtering power improved from 150W to 250W.

Keywords: RF sputtering power, a-axis oriented AlN films, crystal quality, and energy bandgap of AlN.

INTRODUCTIONS

With excellent physical properties such as a high coupling constant, a high melting point, high thermal conductivity, low thermal expansion coefficient high resistivity and wide energy band gap [1], AlN thin films have received considerable interest as a promising candidate for electronic materials for many applications such as dielectric and photoelectric devices [2-3]. To synthesize AlN thin films, a variety of techniques have been used including atomic layer deposition, chemical reaction, magnetron sputtering, and etc [4-5]. Of all, radiofrequency (RF) sputtering offers a controllable film property where various process parameters such as power, pressure, and gas composition of the deposited film can be fine-tuned [6,7]. Besides that, RF sputtering deposition is compatible with a broader range of target materials, including diverse mixtures and alloys [8]. Its higher energy transfer makes for more uniform films, better surface adhesion of target atoms, and higher electron densities, even at low temperatures [9-10].

AlN films prepared with the existing techniques always have several orientations, including the a-axis (100), c-axis (001), (101), (102), and (110) orientations [11-13]. The crystal orientation of aluminium nitride (AlN) significantly impacts its optical properties, influencing factors like refractive index, birefringence, and light transmission. For examples, a-axis AlN films were frequently employed in LED, high-power, and high-frequency electronic devices due to the presence of threading dislocations [3]. When surface roughness exceeds a wavelength in surface acoustic wave (SAW) devices, they may experience an increase in propagation loss or perhaps

stop propagating. Nevertheless, a-axis AlN films with a specific orientation, uniform composition, and minimal surface roughness, offer more favourable conditions for the construction of SAW devices [14]. The facts that fabrication of AlN films with specific crystallographic orientation, is strongly affected by the sputtering system parameters such as i.e. pressure, substrate temperature, target-to-substrate distance, sputtering power, and Ar to N₂ gas mixing ratio, necessitates the effort to study the sputtering conditions on the optical and structural deposited AlN films. Of all parameters, it is reported that, RF magnetron sputtering power significantly impacts the optical and structural properties of AlN thin films (Ref.) At higher powers, the sputtering rate increases, potentially leading to increased defect density and a narrower band gap. Higher power also leads to denser films with higher refractive index and lower extinction coefficient in the visible range [15].

In this work, using RF magnetron sputtering method we synthesized a-axis AlN thin film on Si (100) substrate at room temperature under different RF sputtering power from 150W, 175W, 200W, 225W to 250W. To study the structural and optical properties of the films, X-ray diffraction (XRD) technique and UV-Vis spectroscopy were employed, respectively.

EXPERIMENTAL

AlN thin films were fabricated on Si (100) substrates using RF magnetron sputtering. Since the qualities and characteristics of thin film growth are significantly influenced by the type of substrate used, Si (100) as doped p-type wafers with a $330 \pm 25 \mu\text{m}$ thick and a 0.001-0.002 $\Omega\text{-cm}$ resistivity was chosen as substrate and then were cut into 2 cm x 2 cm. In addition, surface cleaning is a crucial stage in the production of semiconductors as well. The quality and cleanliness of the substrate have a significant effect on the quality of semiconductors thin film. Therefore, the cut samples were degreased with distilled deionized water (DI-Water) and acetone in an ultrasonic bath. To remove organic contaminants from the surface, the wafers were subsequently washed in a 3:1 H₂SO₄ to H₂O solution and then were dried with N₂ gas and ready to be placed in the process chamber. The vacuum chamber was evacuated with turbo molecular and rotary pumps to a base pressure of about 10⁻⁷ torr. The aluminum target with a purity of 99.99% and 2 inches in diameter was utilized as a target. The distance between target to substrate was kept at 10 cm for all samples. The growth parameters such as substrate temperature at room temperature, Ar/N flow ratio at 50/10 sccm, sputtering pressure at 1.7×10^{-3} torr, and deposition time for 60 minutes were kept constants for all samples, but the RF sputtering power were varied from 150W to 250W. The summary of growth parameters is tabulated in Table 1.

TABLE 1. Growth parameters of AlN thin films.

Samples	Power	Target to substrate distance (cm)	Ar/N (sccm)	Sputtering pressure (Torr)	Base Pressure (Torr)	Time (min)
AlN150W	150					
AlN175W	175	10	5	1.7×10^{-3}	2.4×10^{-7}	60
AlN200W	200					
AlN225W	225					
AlN250W	250					

Structural and optical characteristics significantly influence the properties of AlN thin films. UV-Vis's spectroscopy (Shimadzu UV 3600 Plus UV-Vis-MIR) was performed to obtain the absorbance spectra. Then from the absorbance spectra and using Tauc' equation, the bandgap of the films were estimated. The crystal structure and orientation of the films were examined by carrying out the X-ray diffraction (XRD) (Rigaku Smart Lab X-ray diffractometer system).

RESULT AND DISCUSSION

Structural Characterization

To verify the phase identification and crystal structure of the materials, X-ray diffraction (XRD) is utilized as a fundamental instrument and non-destructive experimental procedure. In this study, XRD phase measurement was performed for 2θ range from 20° to 90° using 2θ scan mode to investigate the crystal structure of AlN films in order to analyse the impact of changes in RF sputtering power on the as deposited films. Figure 1 illustrates the X-ray diffraction patterns of AlN films, after baseline correction and normalization. The XRD patterns also revealed two diffraction peaks, located at 2θ values of 52.1° and 53.8° which are attributed to Al_2O_3 and SiO_2 . The oxygen in films as a contaminant from the substrate surface oxidation due to exposing to atmosphere and interaction of high energetic Ar ions with target atoms at presence of ambient oxygen in chamber.

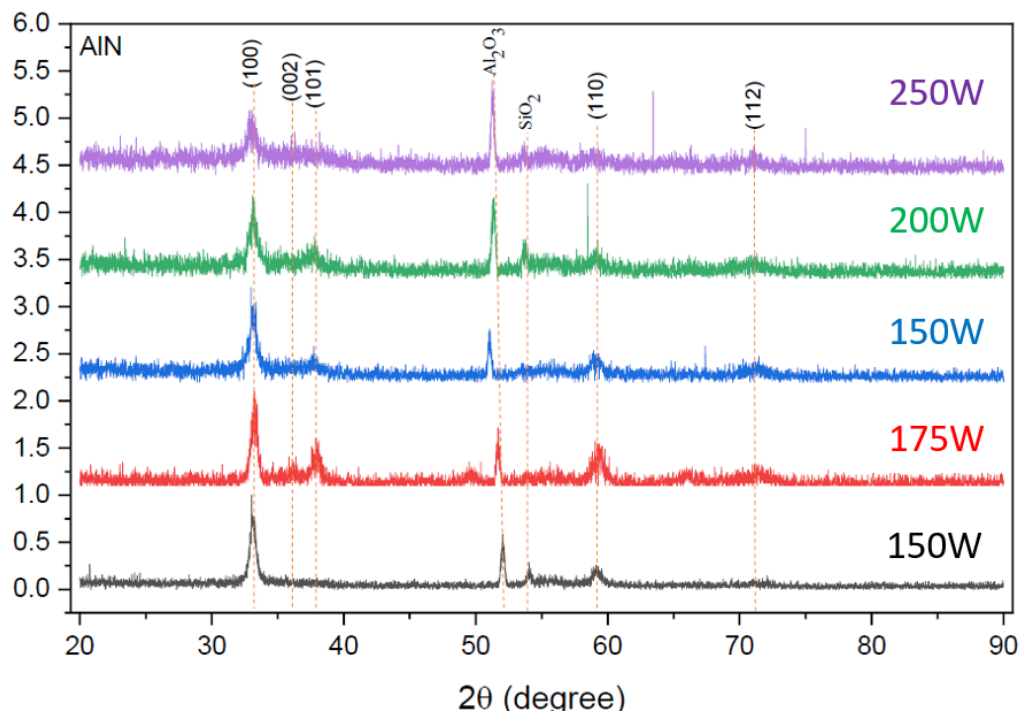


FIGURE 1. XRD pattern of AlN thin film samples synthesized at various RF power

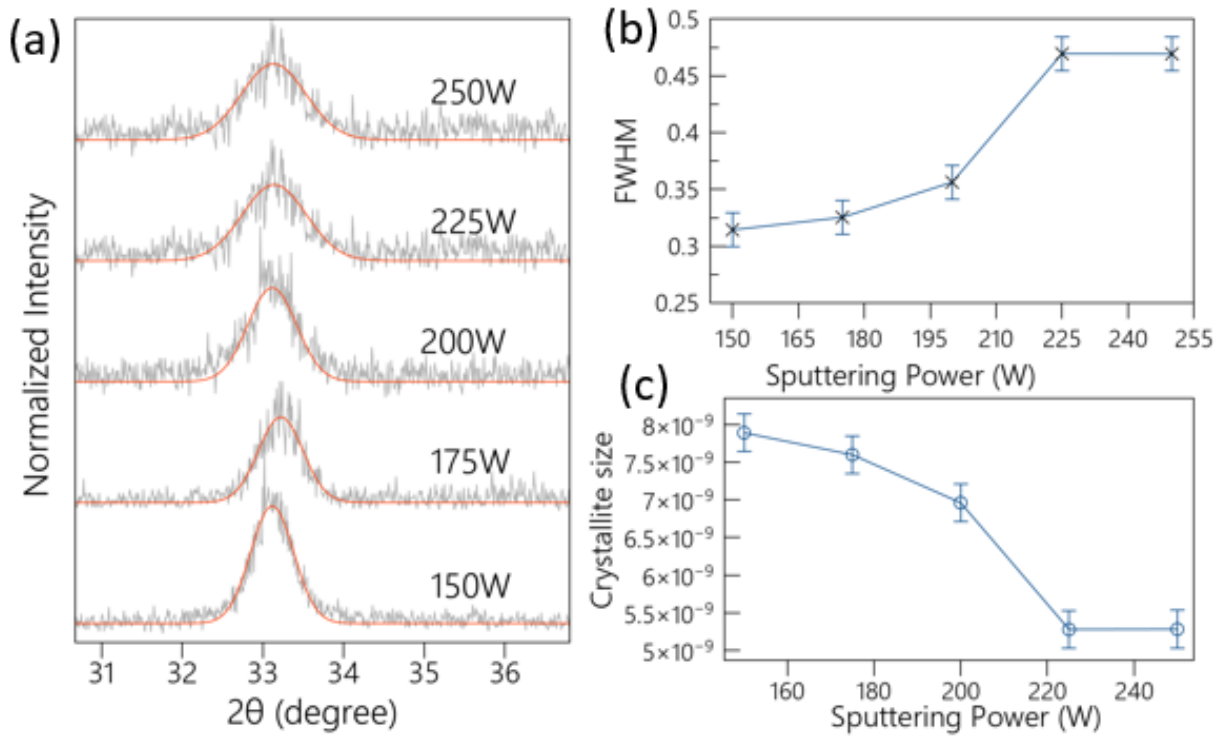


FIGURE 2. Analysis of XRD diffraction peak at 33.33° and correlation with (a) FWHM and (b) crystallite size

All samples indicate the existence of five peaks of AlN at $2\theta=33.17^\circ, 36.29^\circ, 38.24^\circ, 59.08^\circ$ and 71.22° which are corresponding to (100), (002), (101), (110), and (112) planes, respectively. Since the same 2θ peaks have appeared in all samples, therefore this is a strong indication that AlN thin films (all samples as-deposited) possess a polycrystalline structure. As can be clearly observed from Figure 1, there is one prominent AlN peak at $2\theta=33.17^\circ$ which is corresponding to the (100) plane. Based on the results of the analysis, altering the power of sputtering was unable to influence considerably either the crystal orientation or the molecular structure of the film, but could change the peak intensity. The intensity of the prominent peak first incremented but later on decreased as the RF power were increased from 150 W to 250W. Since it is more difficult to construct crystals with high crystal surface energies [3], The energy of ions and atoms increased as RF sputtering power increased. Thus, the peak became more prominent when the sputtering power was increased. The particles' energy became so great with increasing of RF power that led to fabrication of large grains, which caused the crystal orientation to deteriorate [16]. The crystalline size decreases by increasing RF sputtering power. It can be due to the presence of defect and disorder by increasing the Ar ion energy [18]. Two crucial indicators of crystal quality are XRD peak intensity and crystallite size [3]. It was observed that the FWHM of the prominent peak of five samples (AlN150W – AlN250W) are $0.3143^\circ, 0.3253^\circ, 0.3563^\circ, 0.4694^\circ,$ and 0.4693° respectively. As tabulated in Table 2. the value of FWHM increase up to 225W and remain constant at 250 W. The grain size of the films is calculated using Scherrer's equation:

$$\text{Crystallite size} = \frac{k\lambda}{\beta_{hkl}\cos(\theta_{hkl})} \quad (1)$$

where K is the Scherrer constant as derived in Scherrer’s original work where $k=2[\frac{2\ln 2}{\pi}]^{1/2}=0.93$, λ is the X-ray wavelength, β_{hkl} is the FWHM at (hkl) peak radian and θ_{hkl} is the Bragg’s angle for hkl phase. The crystallite size of the films (AlN150W ~ AlN250W) was calculated using the Scherrer equation (Eq 1.) which are 7.890 nm 7.598 nm, 6.961 nm 5.279 nm and 5.282 nm respectively as tabulated in Table 2. As the RF power increased, the crystallite size decreased up to 225W and increased at 250W. These data enabled us to conclude that at 250W of sputtering power, AlN thin films developed more crystals and texture. Higher power provides more energy to sputtered atoms, leading to higher surface mobility and enhancing atomic rearrangement on the substrate. This promotes crystal nucleation and growth, often resulting in improved crystallinity [11].

TABLE 2. XRD phase analysis AlN films as-deposited.

Samples	Peak $2\theta(^{\circ})$	d-value (Å)	h k l	References ICDD	FWHM ($^{\circ}$)	Crystallite Size (nm)
AlN150W	33.11	2.710	100	ICDD: 01-070-2543	0.3143	7.890
AlN175W	33.22	2.695			0.3253	7.598
AlN200W	33.11	2.707			0.3563	6.961
AlN225W	33.14	2.706			0.4694	5.279
AlN250W	33.13	2.708			0.4693	5.282

Optical properties of AlN thin films

UV-Vis’s spectroscopy was employed to obtain the absorbance spectra ranging (from 200 nm to 1000 nm) of AlN films as-deposited. Figure 3 demonstrates the absorbance spectra of the deposited films.

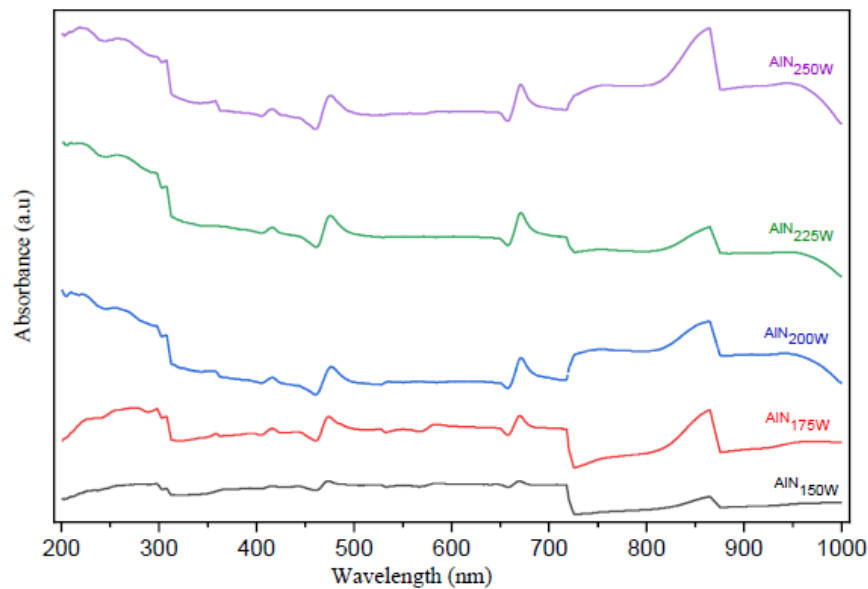


FIGURE 3. Absorbance spectra of AlN films as-deposited

Tauc's plot equation is widely utilized to estimate the band gap of semiconductor material from absorbance spectra, as shown below where $\alpha = 2.303 A/t$ (A is absorbance, and t indicates the thickness of the semiconductor material) is the absorption coefficient, B denotes a constant, $h\nu$ is photon energy, and E_g is 'the bandgap of the semiconductor [17].

$$\alpha h\nu = B(h\nu - E_g)^{1/2} \tag{2}$$

Using the Tauc's plot equation (Eq. 2) and origin software, the optical bandgap energy of the films was estimated from absorbance spectra. Figure 4 shows the Tauc plot to extrapolate the energy band gap of the samples. It was clearly observed that by increasing the RF power from 150W to 250W, the band gap of AlN films also increased. The bandgap of all samples (AlN150W ~ AlN250W) was estimated to increase with RF sputtering power as illustrated in Figure 5. This narrower band gap could be attributed to the existence of nitrogen during the deposition and the presence of oxygen as a contaminant from the substrate surface. AlN films possess a direct bandgap of about 6.2 eV if it is deposited in a vacuum while they exhibited a considerably narrower bandgap when it was synthesized in N₂ ambient and contained oxygen in their composition. AlN crystals often include the impurity oxygen, and prior research has examined how it may affect the growth kinetics and optical properties [18]. This is also consistent with the finding that fabrication of crystalline defects with deep AlN bandgap energy levels occurs when AlN film is deposited at lower temperatures, which reduces the effective forbidden gap [3,19] A narrower optical bandgap than the bulk value can be ascribed to various crystal defects that could cause intermediate energy levels to combine with the conduction band and reduce the band gap [20].

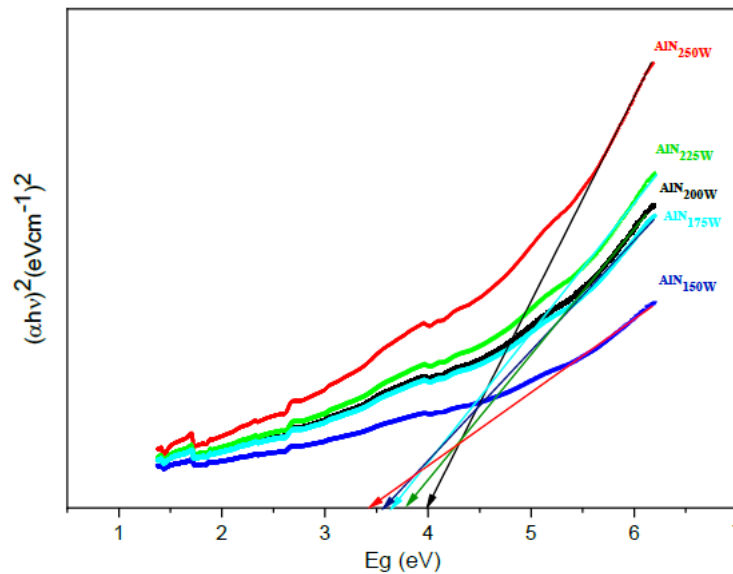


FIGURE 4. Determination of optical bandgap of samples using Tauc plot.

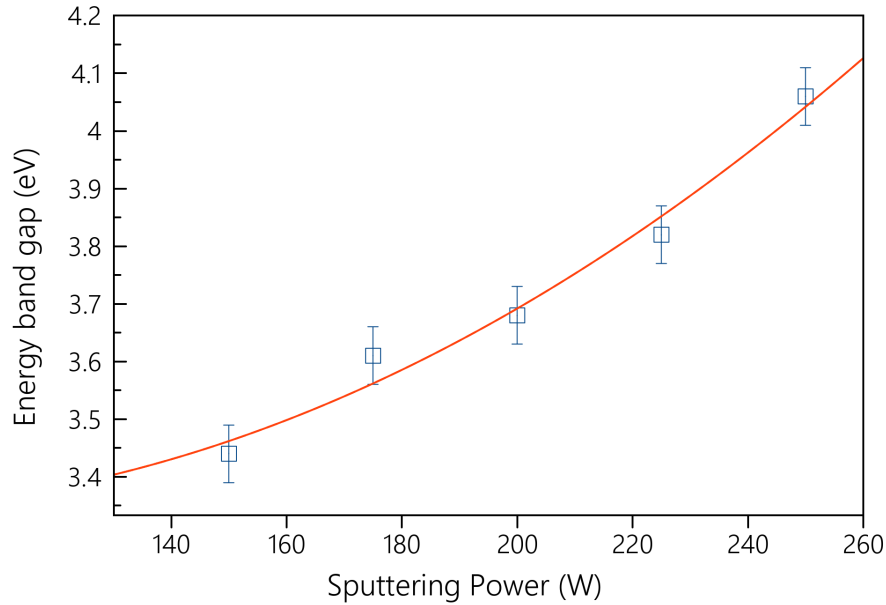


FIGURE 5. Influence of altering RF sputtering power on the energy bandgap of AlN films.

CONCLUSIONS

Using RF magnetron sputtering, AlN thin films were successfully synthesized on the Si wafer at ambient temperature. The influence of RF sputtering power on optical bandgap energy and crystal orientation were examined at various RF power that ranging from AlN150W, AlN175W, AlN200W, AlN225W, to AlN250W. It was observed that, with improve of RF power from 150W to 250W, the optical bandgap energy of AlN films increased from 3.4 eV to 4.0 eV. Using XRD, the crystal structure was examined. XRD results revealed that all AlN thin films revealed five peaks of AlN films at $2\theta = 33.17^\circ$, 36.29° , 38.24° , 59.08° , and 71.22° which are corresponding to (100), (002), (101), (110), and (112) planes, respectively. Since there is only one prominent peak that is at $2\theta = 33.17^\circ$ and corresponding to (100) plane and the rest four peaks are negligible, we considered it as a-axis AlN film. The results revealed that by changing the RF sputtering power, the molecular structure and crystal orientation does not change. But the intensity of the film is altered. The crystalline size decreased, and finally dramatically increased 5.28nm at high sputtering power 250W. These data enabled us to conclude that at 250W of sputtering power, the AlN thin films became more crystalline and textured.

ACKNOWLEDGMENTS

The authors would like to thank the Physics Department, Faculty of Science, University Technology Malaysia (UTM) for providing the fabrication and characterization facilities. The authors also express special thanks to Dr. Mohammad Firdaus Omar and Dr. Alireza Samavati for their fruitful guidance and advice during this study. Authors acknowledge the Ministry of Higher Education (MOHE) for funding under Fundamental Research Grant Scheme FRGS/1/2019/STG02/UTM/02/13 (Vot. No R.J130000.7854.5F243) and UTMFR Grant 21H25 for funding this project.

REFERENCES

1. Fesenko, I. P., Prokopiv, M. M., Chasnyk, V. I., Kaidash, O. M., Oliinik, G. S., & Kuzenkova, M. A. (2015). Aluminum Nitride-Based Functional Materials Obtained from Nanodispersed and Micron Powders by Hot Pressing and Free Sintering.
2. L. Xian Chen *et al.*, “Growth of high-quality AlN films on CVD diamond by RF reactive magnetron sputtering,” *Appl. Surf. Sci.*, vol. 431, pp. 152–159, 2018, doi: 10.1016/j.apsusc.2017.09.036.
3. Y. Lan, Y. Shi, K. Qi, Z. Ren, and H. Liu, “Fabrication and characterization of single-phase a-axis AlN ceramic films,” *Ceram.Int.*, vol. 44, no. 7, pp. 8257–8262, May 2018, doi: 10.1016/j.ceramint.2018.02.007.
4. A. Iqbal and F. Mohd-Yasin, “Reactive sputtering of aluminum nitride (002) thin films for piezoelectric applications: *A review*,” *Sensors (Switzerland)*, vol. 18, no. 6, pp. 1–21, 2018, doi: 10.3390/s18061797.
5. A. Das, M. Rath, D. R. Nair, M. S. Ramachandra Rao, and A. DasGupta, “Realization of preferential (100) oriented AlN thin films on Mo coated Si substrate using reactive RF magnetron sputtering,” *Appl. Surf. Sci.*, vol. 550, no. September 2020, p. 149308, 2021, doi: 10.1016/j.apsusc.2021.149308.
6. N. Redjidal *et al.*, “Indium hexagonal island as seed-layer to boost a-axis orientation of AlN thin films,” *Superlattices Microstruct.*, vol.118, pp. 196–204, 2018, doi: 10.1016/j.spmi.2018.04.015.
7. Z. Liu, H. Wu, W. Ren, and Z.-G. B. T.-R. M. in C. Ye Molecular Sciences and Chemical Engineering, “Piezoelectric and ferroelectric materials: *Fundamentals, recent progress, and applications*,” Elsevier, 2022.
8. C. W. Chung, J. Chun, G. Wang, and W. Um, “Effects of iron oxide on the rheological properties of cementitious slurry,” *Colloids Surfaces A Physicochem. Eng. Asp.*, vol. 453, no. 1, pp. 94–100, 2014, doi: 10.1016/j.colsurfa.2014.03.072.
9. O. Brafman, I. F. Chang, G. Lengyel, S. S. Mitra, and E. Carnall, “Optical phonons in ZnS x Se 1-x mixed crystals,” in *Localized Excitations in Solids*, Springer, 1968, pp. 602–610.
10. Q. Hua, B. Ma, and W. Hu, “Aluminum, Gallium, and Indium Nitrides,” M. B. T.-E. of M. T. C. and G. Pomeroy, Ed. Oxford: Elsevier, 2021, pp. 74–83.
11. E. G. Gillan, “1.31 - Precursor Chemistry – Group 13 Nitrides and Phosphides (Al, Ga, and In),” J. Reedijk and K. B. T.-C. I. C. I. I. (Second E. Poeppelmeier, Eds. Amsterdam: Elsevier, 2013, pp. 969–1000.
12. H. Jin *et al.*, “Influence of substrate temperature on structural properties and deposition rate of AlN thin film deposited by reactive magnetron sputtering,” *Journal of Electronic Materials*, vol. 41, no. 7, pp. 1948–1954, 2012, doi: 10.1007/s11664-012-1999-4.
13. K. Antonova *et al.*, “Influence of laser pulse frequency on the microstructure of aluminum nitride thin films synthesized by pulsed laser deposition,” *Appl. Surf. Sci.*, vol. 394, pp. 197–204, 2017, doi: 10.1016/j.apsusc.2016.10.114.
14. X.-H. Xu, H.-S. Wu, C.-J. Zhang, and Z.-H. Jin, “Morphological properties of AlN piezoelectric thin films deposited by DC reactive magnetron sputtering,” *Thin Solid Films*, vol. 388, no. 1, pp. 62–67, 2001, doi: [https://doi.org/10.1016/S0040-6090\(00\)01914-3](https://doi.org/10.1016/S0040-6090(00)01914-3).
15. Y. Ma *et al.*, “Materials and structure engineering by magnetron sputtering for advanced lithium batteries,” *Energy Storage Mater.*, vol 39, no. February, pp. 203–224, 2021, doi: 10.1016/j.ensm.2021.04.012.

16. Zhang, W. J., & Matsumoto, S. (2000). The effects of dc bias voltage on the crystal size and crystal quality. of cBN films. *Applied Physics A*, 71, 469-472.
17. W. Wei et al., "Temperature dependence of stress and optical properties in aln films grown by mocvd," *Nanomaterials*, vol. 11, no.3, pp. 1–15, 2021, doi: 10.3390/nano11030698.
18. M. Strassburg et al., "The growth and optical properties of large, high-quality AlN single crystals," *J. Appl. Phys.*, vol. 96, no. 10, pp. 5870–5876, 2004, doi: 10.1063/1.1801159.
19. S. Bakalova et al., "VIS/IR spectroscopy of thin AlN films grown by pulsed laser deposition at 400°C and 800°C and various N₂ pressures," *J. Phys. Conf. Ser.*, vol. 514, no. 1, 2014, doi:10.1088/1742-6596/514/1/012001.
20. P. Motamedi and K. Cadien, "Structural and optical characterization of low-temperature ALD crystalline AlN," *J. Cryst. Growth*, vol. 421, pp.45–52, 2015, doi: <https://doi.org/10.1016/j.jcrysgro.2015.04.009.3>.